Journal of Alloys and Compounds 526 (2012) 139–144

Contents lists available at SciVerse ScienceDirect

Journal of Alloys and Compounds

journal homepage: www.elsevier.com/locate/jallcom

The effects of dual doping on the thermoelectric properties of $Ca_{3-x}M_xCo_{4-y}Cu_yO_9$ (M = Na, La)

Y. Ou[a,b,1], J. Peng[a,1], F. Li[c], Z.X. Yu[c], F.Y. Ma[b], S.H. Xie[a,b], J.-F. Li[c], J.Y. Li[b,*]

[a] Faculty of Materials Optoelectronics and Physics, and Key Laboratory of Low Dimensional Materials and Application Technology of Ministry of Education, Xiangtan University, Xiangtan, Hunan 411105, China
[b] Department of Mechanical Engineering, University of Washington, Seattle, WA 98105-2600, USA
[c] State Key Laboratory of New Ceramics and Fine Processing, Department of Materials Science and Engineering, Tsinghua University, Beijing 100084, China

ARTICLE INFO

Article history:
Received 11 November 2011
Received in revised form 17 February 2012
Accepted 17 February 2012
Available online xxx

Keywords:
Thermoelectric oxide
Dual doping
Sol–gel process
Spark plasma sintering

ABSTRACT

The effects of dual doping on the thermoelectric properties of $Ca_{3-x}M_xCo_{3.8}Cu_{0.2}O_9$ (M = Na, La, x = 0.1, 0.2, 0.3) have been systematically investigated, with $Ca_{3-x}M_xCo_{3.8}Cu_{0.2}O_9$ powders synthesized using sol–gel method, and then consolidated into bulk ceramics by spark plasma sintering. It is found that dual doping by Cu and La results in substantial increase in electric conductivity and small decrease in Seebeck coefficient, while dual doping by Cu and Na increase Seebeck coefficient and decrease electric conductivity slightly. Both types of doping enhance power factor and reduce thermal conductivity simultaneously in general, with substantial reduction in thermal conductivity observed in dual doping of Cu and La. These lead to enhancement in thermoelectric figure of merit by both types of doping in general, with ZT value of $Ca_{2.8}La_{0.2}Co_{3.8}Cu_{0.2}O_9$ 78.07% higher than $Ca_3Co_4O_9$ and 57.36% higher than $Ca_3Co_{3.8}Cu_{0.2}O_9$ near 773 K. These results suggest that dual doping by Cu and La is effective in enhancing thermoelectric figure of merit of $Ca_3Co_4O_9$.

1. Introduction

Tremendous amount of waste heat are produced every day, and thermoelectric materials that convert waste heat directly into electricity have received increased attentions [1–3]. For high temperature applications, thermoelectric oxides with excellent thermal stability and oxidation resistance and low toxicity are attractive, though their thermoelectric figure of merit is relatively low. Since the demonstration of the excellent thermoelectric effect in single crystalline $NaCo_2O_4$ [4] and $Ca_3Co_4O_9$, [5] much efforts have been devoted to enhancing the thermoelectric performance of polycrystalline thermoelectric $Ca_3Co_4O_9$, which often exhibits substantially lower figure of merit than single crystals due to their poor electric conductivity [6]. These works can generally be classified into two different though often overlapping approaches. One approach focuses on advanced processing techniques that induce desired textures and nanocrystalline structures in the thermoelectric oxides, including spark plasma sintering (SPS), hot-pressing, multisheet corfiring (MSC), and sol–gel based electrospinning [6–13]. The other approach focuses on partial substitution of cations to adjust the carrier concentrations and thus tune the electric and thermal transport characteristics of thermoelectric oxides. These include using Na, [14,15] Bi, [16,17] Ag, [18–20] La, [21,22] Nd, [23,24] Y, [25] Sr, [26] Gd [27] and Lu [28,29] for the Ca-site doping, which changes the carrier concentration without influencing the band structure much, and Fe, [30,31] Cu, [30,31] Ga, [32] Zn, [33] Mn, [30,31] Ag, [34] Ti, [35] Ni, [31] for the Co-site doping, which can cause changes in both band structure and transport mechanism [36–38].

By surveying the available data in literature on the effects of doping in $Ca_3Co_4O_9$, it was noticed that Co-site doping by Cu has resulted in one of the highest electric conductivities in $Ca_3Co_4O_9$ based system, with conductivity of 163.4 S/cm achieved in $Ca_3Co_{3.8}Cu_{0.2}O_9$ at 1000 K [31]. On the other hand, one of the highest Seebeck coefficients of 274 μV/K has been achieved in Ca-site doping by Na, obtained in $Ca_{2.85}Na_{0.05}Co_4O_9$ at 1054 K, [39] though its electric conductivity is rather low, measured to be only 33.6 S/cm. This motivated us to examine the effects of Ca-site doping by Na and Co-site doping by Cu simultaneously, so that both Seebeck coefficient and electric conductivity of $Ca_3Co_4O_9$ can be enhanced. Furthermore, we also explored Ca-site doping by La instead of Na, which has been shown to possess both excellent electric conductivity (213 S/cm) and good Seebeck coefficient (156 μV/K) at 975 K [22]. While dual substitutions at both Ca-site and Co-site have been investigated before, particularly Ca-site by Bi and Co-site by Cu, [40,41] the resulting electric conductivity is relatively low, measured to be 103 S/cm at 1000 K, and

* Corresponding author.
E-mail address: jjli@uw.edu (J.Y. Li).
[1] These authors contributed equally to the work.

0925-8388/$ – see front matter © 2012 Elsevier B.V. All rights reserved.
doi:10.1016/j.jallcom.2012.02.112

Table 1
$Ca_{3-x}M_xCo_{4-y}Cu_yO_9$ samples with different doping and compositions.

Doping	Chemical formula	Abbreviation
Co-site doping by Cu	$Ca_3Co_4O_9$	CCO
	$Ca_3Co_{3.8}Cu_{0.2}O_9$	CCCO
Dual doping by Cu and Na	$Ca_{2.8}Na_{0.2}Co_{3.8}Cu_{0.2}O_9$	CNCCO-2
	$Ca_{2.7}Na_{0.3}Co_{3.8}Cu_{0.2}O_9$	CNCCO-3
Dual doping by Cu and La	$Ca_{2.9}La_{0.1}Co_{3.8}Cu_{0.2}O_9$	CLCCO-1
	$Ca_{2.8}La_{0.2}Co_{3.8}Cu_{0.2}O_9$	CLCCO-2
	$Ca_{2.7}La_{0.3}Co_{3.8}Cu_{0.2}O_9$	CLCCO-3

substantial grain growth has also been observed that is not desirable for the reduction of thermal conductivity, which we hope to avoid by using Na or La instead of Bi.

2. Experimental procedures

$Ca_{3-x}M_xCo_{4-y}Cu_yO_9$ powders with different doping and compositions have been synthesized by sol–gel method, as summarized in Table 1. Stoichiometric proportions of $Ca(NO_3)_2{\cdot}3H_2O$, $Co(NO_3)_2{\cdot}6H_2O$, $Cu(NO_3)_2{\cdot}3H_2O$, $C_6H_5Na_3O_7{\cdot}2H_2O$ and $LaNO_3{\cdot}6H_2O$ were dissolved in an aqueous solutions of citric acid first, with the molar ratio of cations to $C_6H_8O_7$ kept to be 1:1.1. Polyethylene glycol (PEG) 400 was then added to the sol–gel precursors with its volume ratio controlled to be 0.2%, and ammonia was also added to control the pH value of the solutions to be around 1.0–2.0. The mixture solutions were stirred continuously to form 1.0 mol/L homogeneous precursors. The precursors were heated at 80 °C for 24 h before dried at 120 °C for 12 h to obtain xerogel, followed by calcinating the xerogel at 750 °C for 4 h in air. These powders were then consolidated into bulk ceramics by SPS, and the details of SPS process was described in our earlier work [12].

The crystalline structure of sol–gel powders was characterized by X-ray diffraction (XRD, RigaKu D/max 2500VB+) with Cu Kα radiation (λ = 0.15406 nm), and the morphologies of sol–gel powders and SPS specimens were examined by scanning electron microscopy (SEM, JSM-6700F). The element doping was examined by X-ray photoelectron spectroscopy (XPS, K-Alpha 1063). The Seebeck coefficient and electrical resistivity of the SPS specimens were measured using a Seebeck coefficient/electric resistance measuring system (ZEM-2, Ulvac-Riko, Japan), and the thermal diffusivity was measured by the laser flash method (NETZSCH, LFA427, Germany). The specific heat was measured using a thermal analyzing apparatus (Dupont 1090B, USA), and the density of the sample was measured by the Archimedes method. The thermal conductivity was calculated from the product of thermal diffusivity, specific heat and density.

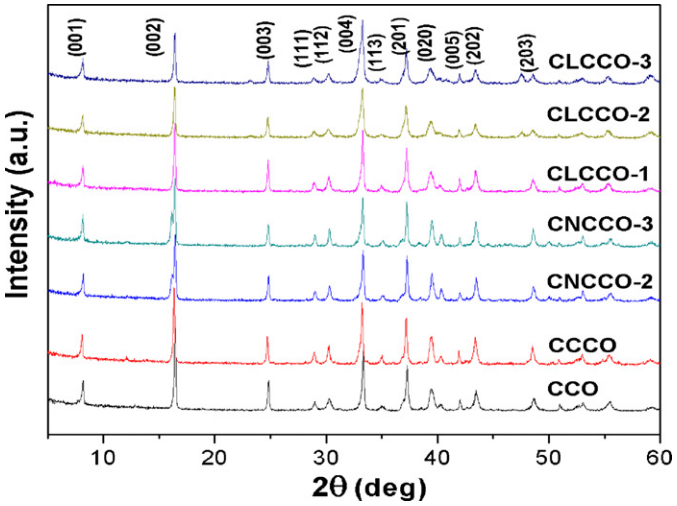

Fig. 1. XRD patterns of $Ca_{3-x}M_xCo_{4-y}Cu_yO_9$ powders with different doping and compositions.

3. Results and discussion

3.1. Microstructures

The crystalline structures of $Ca_{3-x}M_xCo_{4-y}Cu_yO_9$ powders of different doping and compositions were examined by XRD before SPS sintering, as shown in Fig. 1. From standard PDF Card (No.58-0661), it is determined that all the diffraction peaks of these powders are consistent with polycrystalline $Ca_3Co_4O_9$, though the existence of $Ca_9Co_{12}O_{28}$ cannot be excluded, since its peaks are essentially identical to those of $Ca_3Co_4O_9$ according to standard PDF Card (No. 21-0139). After SPS sintering, the morphologies of

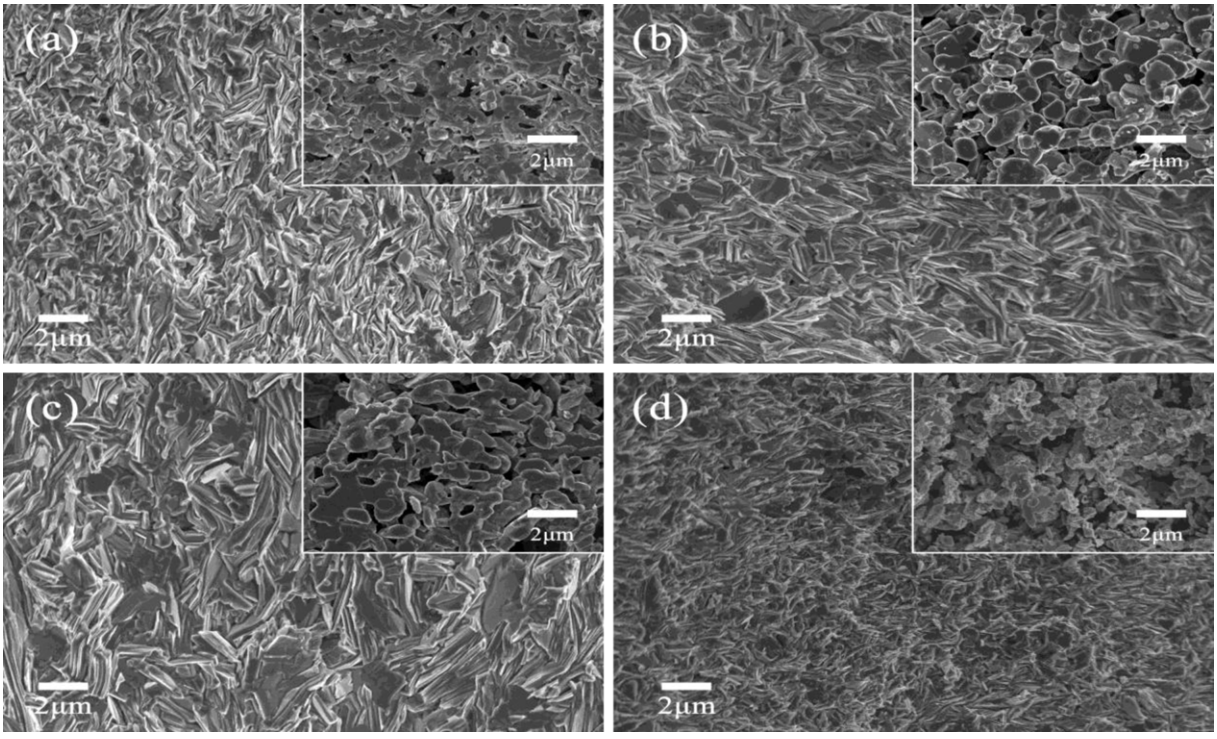

Fig. 2. SEM images of $Ca_{3-x}M_xCo_{4-y}Cu_yO_9$ specimens with different doping and compositions; (a) CCO; (b) CCCO; (c) CNCCO-2; and (d) CLCCO-2.

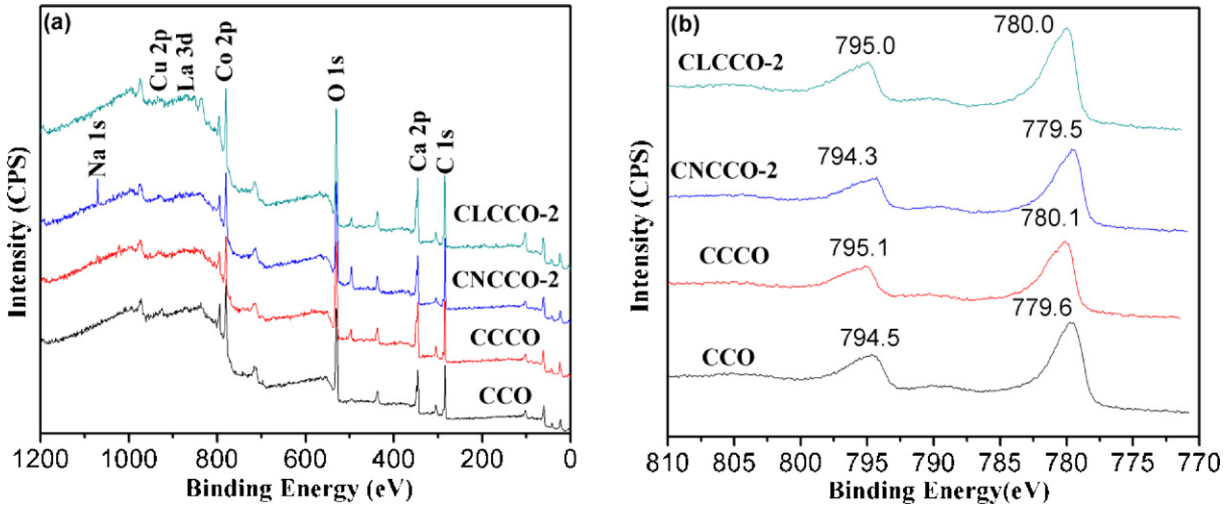

Fig. 3. XPS patterns of $Ca_{3-x}M_xCo_{4-y}Cu_yO_9$ powders with different doping and compositions; (a) XPS survey spectra of doped $Ca_3Co_4O_9$; and (b) XPS Co2p spectra of doped $Ca_3Co_4O_9$.

$Ca_{3-x}M_xCo_{4-y}Cu_yO_9$ specimens with different doping and compositions were examined by SEM, as shown in Fig. 2 for four representative specimens, with the corresponding SEM images of sol–gel powders in the inset. It is observed that the sol–gel synthesized powders are relatively loose, have particle sizes in the range of 0.5–2 μm. After SPS, much more dense structure with lamellar grains is observed in all the specimens, and there are no obvious differences in grain size among most specimens after SPS, though the grain size of CLCCO-2 (Fig. 2(d)) appears to be notably smaller, and the corresponding powder size shown in the inset also appears to be finer. The dense structure is also confirmed by density measurement after SPS, ranging from 93.3% to 98.8% of theoretical density of 4.94 g/cm^3 [42].

To verify the doping of various elements, we carried out XPS studies, as shown in Fig. 3. The XPS survey spectra of $Ca_{3-x}M_xCo_{4-y}Cu_yO_9$ with four different compositions are shown in Fig. 3(a), where Cu2p is observed at 933 eV, Na1s at 1071 eV, and La3d at 835 eV and 855 eV. These confirm doping of Cu, Na, and La in specimens of respective compositions. To understand the effects of doping, we have also checked Co2p spectra of these four specimens in details, as shown in Fig. 3(b). The peaks of $Co2p_{3/2}$ of CCO, CCCO, CNCCO-2, CLCCO-2 are 779.6 eV, 780.1 eV, 779.5 eV and 780.0 eV, respectively, indicating that the binding energy increases notably with Cu doping and Cu and La dual doping, and decrease slightly with Cu and Na dual doping. The higher binding energy in CCCO and CLCCO-2 suggests that there are fewer bound charges in doped sites. Since the peaks of $Co2p_{3/2}$ in CoO and Co_2O_3 are 780.4 eV and 779.9 eV, [43] respectively, increased binding energy toward 780.4 eV suggests that Co is shifted from high valence Co^{3+} to low valence Co^{2+} by doping of Cu and La, and this could result in higher carrier (hole) concentration that influence electric conduction and thermopower, as we discuss next.

3.2. Thermoelectric properties

The Seebeck coefficient S as a function of temperature for $Ca_{3-x}M_xCo_{4-y}Cu_yO_9$ specimens with different doping and compositions is shown in Fig. 4(a), and all the values are positive, consistent with p-type semiconductors. It is observed that Na-doping increases the Seebeck coefficient, while La-doping decreases it, though the changes are rather small in both directions. CNCCO-3 has the highest Seebeck coefficient at high temperature, measured to be 168 μV/K at 873 K, consistent with report in Ref. [14]. This represents only 3.19% enhancement over CCO and 5.07% enhancement over CCCO. On the other hand, the Seebeck coefficient of CLCCO-3 is substantially reduced, and is lowest among all the specimens we studied, presumably due to their increased carrier concentration as indicated by XPS, where it is observed that doping by Cu and La shift high valence Co^{3+} to low valence Co^{2+}. The electrical conductivity of $Ca_{3-x}M_xCo_{4-y}Cu_yO_9$ specimens as a function of temperature is shown in Fig. 4(b), and it is observed that the electric conductivity increases with temperature in general, typical for semiconductors. At relatively low temperatures, the decrease with electric conductivity is also observed in CCO and CCCO specimens, which could be caused by a spin-state transition of Co ions around 420 K [44]. The electrical conductivity of CCCO is larger than CCO by the rise of the hole concentration originated from the substitution of Cu^{2+} for Co^{3+} [41], which is consistent with previously report [31]. The conductivities of CLCCO-1 and CLCCO-2 are slightly smaller than CCCO, because the substitution of La^{3+} for Ca^{2+} decreases hole concentration, while that of CLCCO-3 is larger than CCO, presumably due to valance change of Co resulted from higher doping of La as suggested by XPS. This could also explain the slight reduction in conductivity associated with Na doping, which slightly reduces the binding energy of Co according to XPS spectra, and such reduction has also been reported before [39]. Such decrease might also be due to the reduced carrier mobility by Na doping [14]. It is worth to point out that the electric conductivity of CLCCO-3 is one of the highest among all the literature data we surveyed, reaching 178.4 S/cm at 873 K, 37% higher than that of CCO and 24% higher than CCCO. CNCCO-3, on the other hand, has the lowest electric conductivity. The opposite effects of doping on Seebeck coefficient and electric conductivity highlights the difficulty in enhancing thermoelectric properties, wherein high electric conductivity requires high carrier concentration, which is not optimal for Seebeck coefficient. Indeed, the power factors $P = \sigma S^2$ as a function of temperature for $Ca_{3-x}M_xCo_{4-y}Cu_yO_9$ specimens are shown in Fig. 4(c), and it is observed that CLCCO-1, which has modest electric conductivity and Seebeck coefficient, shows the highest power factor, calculated to be 3.83×10^{-4} W/mK^2 at 873 K, 11.34% higher than CCO and 4.36% higher than CCCO.

The thermal diffusivity D as a function of temperature for $Ca_{3-x}M_xCo_{4-y}Cu_yO_9$ specimens with different doping and compositions is shown in Fig. 5(a), and it is observed that they all decreases monotonously with temperature, showing typical thermal conduction behavior of crystalline semiconductors. It is evident that dual doping by heavy elements such as Cu and La decreases the thermal diffusivity of CLCCO compared to both CCO and CCCO, while doping

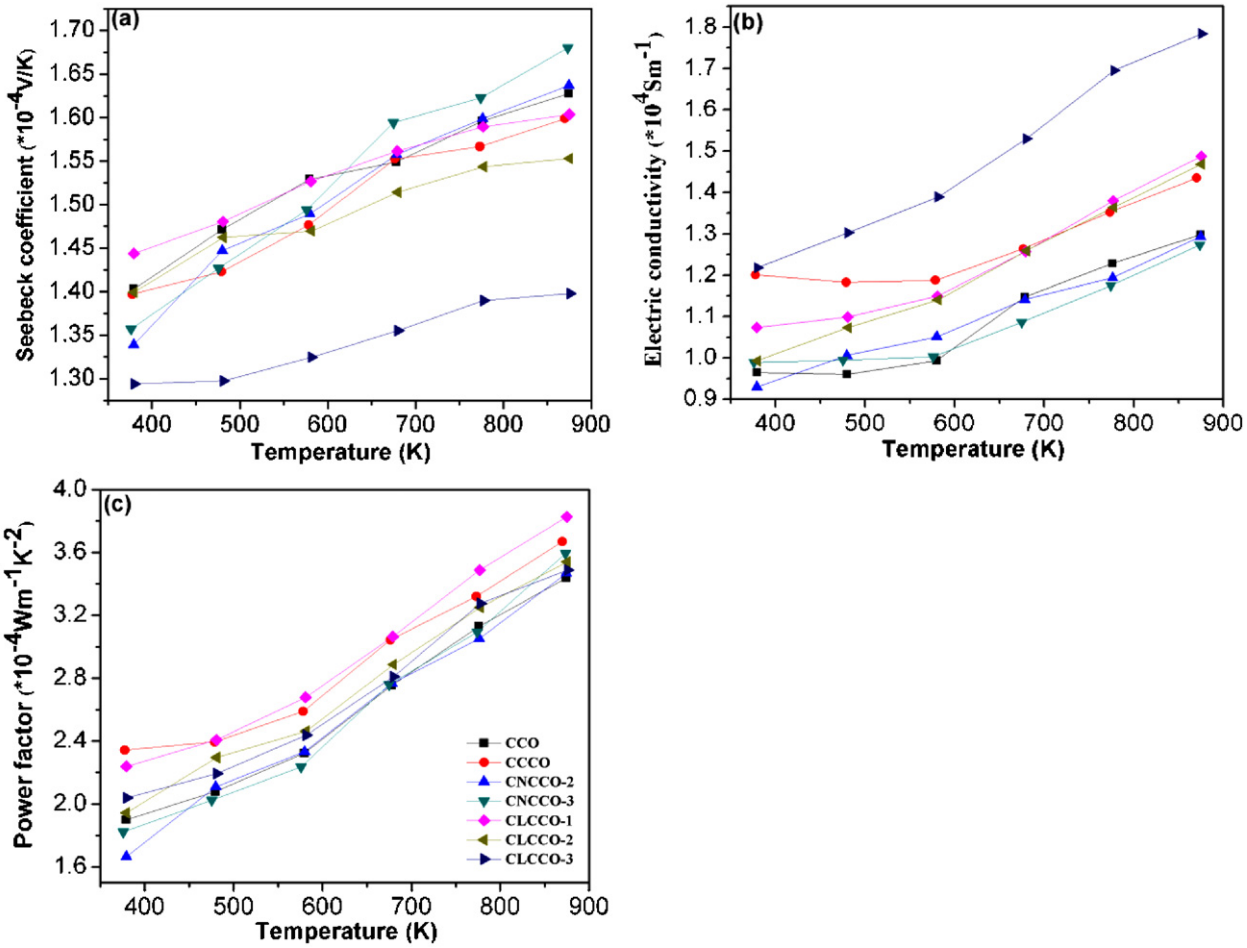

Fig. 4. Thermoelectric properties of $Ca_{3-x}M_xCo_{4-y}Cu_yO_9$ specimens with different doping and compositions; (a) Seebeck coefficient; (b) electrical conductivity; and (c) power factor.

by light element Na increases the thermal diffusivity. The thermal diffusivity of CLCCO-1 is lowest, measured to be 4.70×10^{-3} cm^2/s at 873 K, 8.74% lower than that of CCO and 1.26% lower than that of CCCO. The specific heat capacity *Cp* as a function of temperature for $Ca_{3-x}M_xCo_{4-y}Cu_yO_9$ specimens is shown in Fig. 5(b), and it is observed that it increases at low temperature initially, and then decreases between 373 K and 523 K, after which the heat capacity increases again. In general, the heat capacity decreases with the doping, though there is no clear trend on the effect of various doping elements, and this is under further investigation. The thermal conductivity $\kappa = \rho DCp$ as a function of temperature is shown in Fig. 5(c), where ρ is the density of the specimens. It is observed that although the thermal diffusivity decreases with the increased temperature, the thermal conductivity decreases with temperature initially, and then increases at high temperature caused by the increased heat capacity *Cp*. It is interesting to note that all the doping decreases the thermal conductivity in general, presumably due to enhanced phonon scatterings.

It is well known that the thermal conductivity of a material can be decomposed into phonon contribution κ_{ph} and electronic contribution κ_e, and according to the Wiedemann–Franz law, [45] $\kappa_e = L\sigma T$ where $L = 2.44 \times 10^{-8}$ V^2/K^2 is the Lorentz constant [46]. Using this formula, we evaluated the electronic contribution to thermal conductivity for various doping, from which we can conclude that the thermal conductivity of $Ca_{3-x}M_xCo_{4-y}Cu_yO_9$ is dominated by phonons, and electronic term only contributes a small fraction to it. This can help us to understand the trend in Fig. 5(c), where the substitution of heavy elements such as Cu and La increases phonon scattering, and thus decrease the thermal conductivity considerably [14,30]. CLCCO-2 has the lowest thermal conductivity measured to be 1.627 W/mK at 873 K, which is 30.32% lower than that of CCO and 27.71% lower than CCCO, and is one of the lowest among the literature data we surveyed. In addition to the effects of doping on phonon scattering, the grain size, which is smallest for CLCCO-2 based on SEM images in Fig. 2, might also play a role here.

The thermoelectric figure of merit $ZT = \sigma S^2/\kappa$ as a function of temperature for $Ca_{3-x}M_xCo_{4-y}Cu_yO_9$ specimens with different doping and compositions is shown in Fig. 6(a), and it is evident that the thermoelectric figure of merit is improved for all these doping and compositions in general, and dual doping by La and Cu is more effective than single doping by Cu and dual doping by Na and Cu. Among all the specimens, CLCCO-2 has the highest *ZT*, reaching 0.203 near 773 K, representing 78.07% increase over CCO and 57.36% over CCCO at 773 K. This is due to its simultaneous high electric conductivity and low thermal conductivity, even though its Seebeck coefficient is modest. Slight decrease of *ZT* is observed in CLCCO-2 after 773 K due to sharp rise in thermal conductivity as observed in Fig. 5(c), though it is still 47.66% higher than CCO and 33.10% higher than CCCO at 873 K. For dual doped specimens with Na and Cu, *ZT* enhancement is modest at most temperatures, and CNCCO-3 has a relatively high *ZT* of 0.158 at 873 K, which is 23.44% higher than CCO at the same temperature and is mainly due to its high Seebeck coefficient at high temperatures.

To put our investigation into broader context, we also compare the *ZT* of our $Ca_{3-x}M_xCo_{4-y}Cu_yO_9$ specimens at 773 K

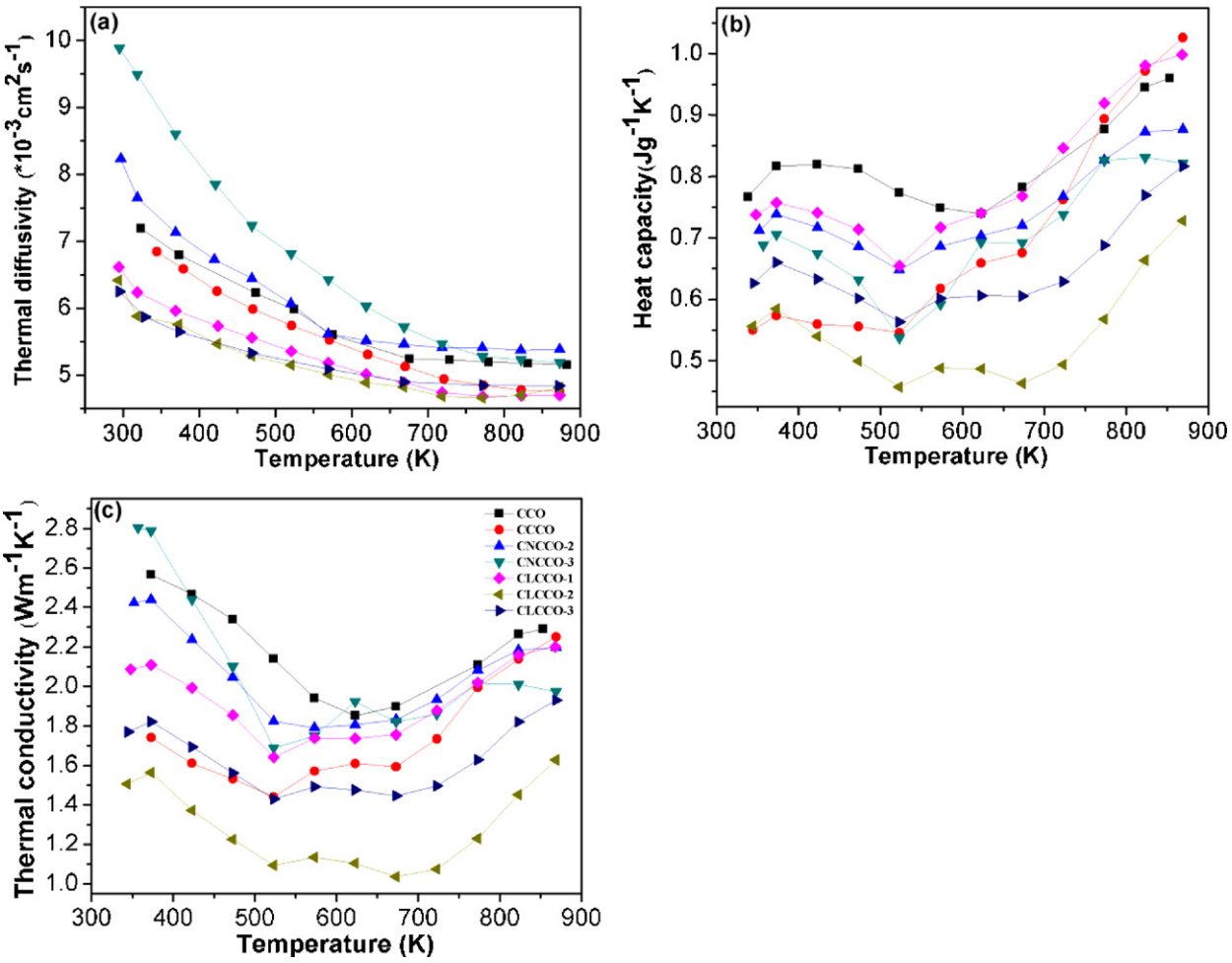

Fig. 5. Thermal conductivity as functions of temperature for $Ca_{3-x}M_xCo_{4-y}Cu_yO_9$ specimens with different doping and compositions; (a) thermal diffusivity; (b) heat capacity; and (c) thermal conductivity.

with available data in literature on other doped $Ca_3Co_4O_9$ systems, including Co-site doping in $Ca_3Co_{3.95}Zn_{0.05}O_9$, [33] $Ca_3Co_{3.9}Mn_{0.1}O_9$, [30] $Ca_3Co_{3.9}Cu_{0.1}O_9$, [30] $Ca_3Co_{3.8}Ag_{0.2}O_9$, [34] $Ca_3Co_{3.7}Ti_{0.3}O_9$, [35] and $Ca_3Co_{3.9}Fe_{0.1}O_9$, [30] Ca-site doping in $Ca_{2.5}Na_{0.5}Co_4O_9$, [14] $Ca_{2.8}Pr_{0.2}Co_4O_9$, [47] $Ca_{2.7}Y_{0.3}Co_4O_9$, [25] $Ca_{2.85}Bi_{0.15}Co_4O_9$, [16] $Ca_{2.7}Er_{0.3}Co_4O_9$, [48] $Ca_{2.7}Eu_{0.3}Co_4O_9$, [49] and dual doping of Ca- and Co-sites in such as $Ca_{2.6}Nd_{0.3}Na_{0.1}Co_4O_9$, [23] $Ca_{2.7}Gd_{0.15}Y_{0.15}Co_4O_9$, [46] $Ca_{2.8}Ba_{0.1}Ag_{0.1}Co_4O_9$, [19] and $Ca_{2.4}Bi_{0.3}Na_{0.3}Co_4O_9$, [15] as shown in Fig. 6(b). It is clear that the *ZT* of CLCCO-2, being 0.203 at 773 K, is one of the highest among data reported in literature. Substantial improvement in *ZT* value by dual doping of Cu and La is observed compared to dual doping by other elements, and the *ZT* value of CLCCO-2 is slightly higher than Co-site doping by Fe, which is highly textured using a high pressure

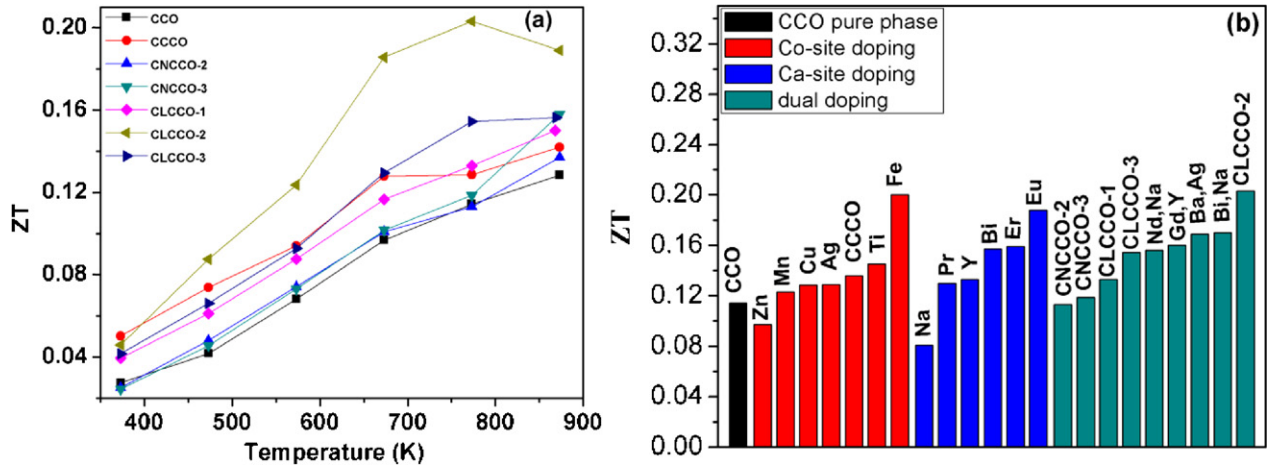

Fig. 6. Thermoelectric figure of merit *ZT* of $Ca_3Co_4O_9$ with different doping and compositions; (a) *ZT* as a function of temperature for $Ca_{3-x}M_xCo_{4-y}Cu_yO_9$ specimens with different doping and compositions; and (b) comparison of *ZT* values with different doping at 773 K reported in literature.

cold press, and show rather high Seebeck coefficient of 257.3 μV/K at 1000 K [30]. Dual doping using Fe at Ca-site is currently under investigation. It is also noted that *ZT* value of 0.61 has recently been reported in $Ca_{2.8}Ag_{0.05}Lu_{0.15}Co_4O_9$ at 1118 K [50], though this is actually a nanocomposite consisting of metallic Ag nanoinclusion, and thus it is not included in the comparison of effects of doping.

4. Conclusions

In conclusion, we have synthesized polycrystalline $Ca_{3-x}M_xCo_{3.8}Cu_{0.2}O_9$ (M = Na, La, $x = 0.1$, 0.2, 0.3) ceramics using sol–gel method followed by spark plasma sintering, and have systematically investigated their thermoelectric properties. It is found that dual doping by Cu and La leads substantial increase in electric conductivity and reduction in thermal conductivity substantially, with only small decrease in Seebeck coefficient. These results in substantial enhancement in thermoelectric figure of merit, with *ZT* value reaching 0.203 $Ca_{2.8}La_{0.2}Co_{3.8}Cu_{0.2}O_9$ near 773 K, one of the highest among data reported in literature in for $Ca_3Co_4O_9$ based systems in this temperature range, suggesting that dual doping by Cu and La is effective in enhancing thermoelectric figure of merit of $Ca_3Co_4O_9$.

Acknowledgments

We acknowledge support from National Science Foundation (CMMI-0969543) and Natural Science Foundation of China (Approval No. 1117225 and Approval No. 51172189). Y. Ou and S.H. Xie also acknowledge partial support of China Scholarship Council.

References

[1] G.J. Snyder, E.S. Toberer, Nat. Mater. 7 (2008) 105.
[2] H. Ohta, K. Sugiura, K. Koumoto, Inorg. Chem. 47 (2008) 8429.
[3] A.J. Minnich, M.S. Dresselhaus, Z.F. Ren, G. Chen, Energy Environ. Sci. 2 (2009) 466.
[4] I. Terasaki, Y. Sasago, K. Uchinokura, Phys. Rev. B 56 (1997) 12685.
[5] M. Shikano, R. Funahashi, Appl. Phys. Lett. 82 (2003) 1851.
[6] D. Kenfaui, G. Bonnefont, D. Chateigner, G. Fantozzi, M. Gomina, J.G. Noudem, Mater. Res. Bull. 45 (2010) 1240.
[7] Y.H. Liu, Y.H. Lin, Z. Shi, C.W. Nan, Z.J. Shen, J. Am. Ceram. Soc. 88 (2005) 1337.
[8] O.J. Kwon, W. Jo, K.E. Ko, J.Y. Kim, S.H. Bae, H. Koo, S.M. Jeong, J.S. Kim, C. Park, J. Mater. Sci. 46 (2011) 2887.
[9] Y.F. Zhang, J.X. Zhang, Q.M. Lu, Ceram. Int. 33 (2007) 1305.
[10] J.G. Noudem, M. Prevel, A. Veres, D. Chateigner, J. Galy, J. Electroceram. 22 (2009) 91.
[11] Y. Masuda, D. Nagahama, H. Itahara, T. Tani, W.S. Seoc, K. Koumotoa, J. Mater. Chem. 13 (2003) 1094.
[12] T.F. Yin, D.W. Liu, Y. Ou, F.Y. Ma, S.H. Xie, J.F. Li, J.Y. Li, J. Phys. Chem. C 114 (2010) 10061.
[13] J.G. Noudem, J. Eur. Ceram. Soc. 29 (2009) 2659.
[14] G.J. Xu, R. Funahashi, M. Shikano, Q.R. Pu, B. Liu, Solid State Commun. 124 (2002) 73.
[15] G.J. Xu, R. Funahashi, M. Shikano, I. Matsubara, Y.Q. Zhou, Appl. Phys. Lett. 80 (2002) 3760.
[16] Y.H. Liu, Y.H. Lin, L. Jiang, C.W. Nan, Z.J. Shen, J. Electroceram. 21 (2008) 748.
[17] Y. Song, Q. Sun, L.R. Zhao, F.P. Wang, Key Eng. Mater. 434 (2010) 393.
[18] F.P. Zhang, Q.M. Lu, J.X. Zhang, X. Zhang, J. Alloys Compd. 477 (2009) 543.
[19] F.P. Zhang, Q.M. Lu, J.X. Zhang, J. Alloys Compd. 484 (2009) 550.
[20] Y. Wang, Y. Sui, J.G. Cheng, X.J. Wang, W.H. Su, J. Alloys Compd. 477 (2009) 817.
[21] J. Nan, J. Wu, Y. Deng, C.W. Nan, Solid State Commun. 124 (2002) 243.
[22] Y.H. Lin, J.L. Lan, Z.J. Shen, Y.H. Liu, C.W. Nan, J.F. Li, Appl. Phys. Lett. 94 (2009) 072107.
[23] J. Pei, G. Chen, D.Q. Lu, P.S. Liu, N. Zhou, Solid State Commun. 146 (2008) 283.
[24] M. Prevel, E.S. Reddy, O. Perez, W. Kobayashi, I. Terasaki, C. Goupil, J.G. Noudem, Jpn. J. Appl. Phys. 46 (2007) 6533.
[25] H.Q. Liu, Y. Song, S.N. Zhang, X.B. Zhao, F.P. Wang, J. Phys. Chem. Solids 70 (2009) 600.
[26] F. Delorme, C.F. Martin, P. Marudhachalam, D. Ovono Ovono, G. Guzman, J. Alloys Compd. 509 (2011) 2311.
[27] G.D. Tang, C.P. Tang, X.N. Xu, Y. He, L. Qiu, L.Y. Lv, Z.H. Wang, Y.W. Du, J. Electron. Mater. 40 (2011) 504.
[28] G.D. Tang, Z.H. Wang, X.N. Xu, L. Qiu, L. Xing, Y.W. Du, J. Mater. Sci. 45 (2010) 3969.
[29] N.V. Nong, C.J. Liu, M. Ohtaki, J. Alloys Compd. 509 (2011) 977.
[30] Y. Wang, Y. Sui, X.J. Wang, W.H. Su, X.Y. Liu, J. Appl. Phys. 107 (2010) 033708.
[31] Q. Yao, D.L. Wang, L.D. Chen, X. Shi, M. Zhou, J. Appl. Phys. 97 (2005) 103905.
[32] N.V. Nong, C.J. Liu, M. Ohtaki, J. Alloys Compd. 491 (2010) 53.
[33] W. Wong-Ng, T. Luo, W. Xie, W.H. Tang, J.A. Kaduk, Q. Huang, Y. Yan, S. Chattopadhyay, X. Tang, T. Tritt, J. Solid State Chem. 184 (2011) 2159.
[34] L. Han, Y. Jiang, S.Y. Li, H.M. Su, X.Z. Lan, K.X. Qin, T.T. Han, H.H. Zhong, L. Chen, D.B. Yu, J. Alloys Compd. 509 (2011) 8970.
[35] L.X. Xu, F. Li, Y. Wang, J. Alloys Compd. 501 (2010) 115.
[36] R. Asahi, J. Sugiyama, T. Tani, Phys. Rev. B 66 (2002) 155103.
[37] I. Terasaki, I. Tsukada, Y. Iguchi, Phys. Rev. B 65 (2002) 195106.
[38] T. Takeuchi, T. Kondo, T. Takami, H. Takahashi, H. Ikuta, U. Mizutani, K. Soda, R. Funahashi, M. Shikano, M. Mikami, S. Tsuda, T. Yokoya, S. Shin, T. Muro, Phys. Rev. B 69 (2004) 125410.
[39] J. Nan, J. Wu, Y. Deng, C.W. Nan, J. Eur. Ceram. Soc. 23 (2003) 859.
[40] K. Iwasakia, H. Yamaneb, J. Takahashic, S. Kubotac, T. Nagasakid, Y. Aritaa, Y. Nishia, T. Matsuia, M. Shimada, J. Phys. Chem. Solids 66 (2005) 303.
[41] H.S. Hao, L.M. Zhao, X. Hu, J. Mater. Sci. Technol. 25 (2009) 105.
[42] I. Matsubara, R. Funahashi, T. Takeuchi, S. Sodeoka, J. Appl. Phys. 90 (2001) 462.
[43] J.F. Moulder, W.F. Stickle, P.E. Sobal, Handbook of X-ray Photoelectron Spectroscopy, Physical Electronics Inc., 1995, p. 82.
[44] A.C. Masset, C. Michel, A. Maignan, M. Hervieu, O. Toulemonde, F. Studer, B. Raveau, J. Hejtmanek, Phys. Rev. B 62 (2000) 166.
[45] G.V. Chester, A. Thellung, Proc. Phys. Soc. 77 (1961) 1005.
[46] H.Q. Liu, X.B. Zhao, T.J. Zhu, Y. Song, F.P. Wang, Curr. Appl. Phys. 9 (2009) 409.
[47] F.P. Zhang, X. Zhang, Q.M. Lu, J.X. Zhang, Y.Q. Liu, G.Z. Zhang, Solid State Sci. 13 (2011) 1443.
[48] J. Pei, G. Chen, N. Zhou, D.Q. Lu, F. Xiao, Physica B 406 (2011) 571.
[49] D.L. Wang, L.D. Chen, Q. Yao, J.G. Li, Solid State Commun. 129 (2004) 615.
[50] N.V. Nong, N. Pryds, S. Linderoth, M. Ohtaki, Adv. Mater. 23 (2011) 2484.